Techniques for the Compensation for Chromatic-Dispersion Effects in Fiber-Wireless Systems

D. Hervé, J.L. Corral
J.M. Fuster, J. Herrera,
A. Martinez, V. Polo
F. Ramos, E. Vourc'h
J. Marti

1. Introduction

Fibre-wireless systems have been extensively studied over the past years with a view towards the development of broadband-access solutions [1-3]. In such networks, base stations can be made simple and compact when the radio-frequency (RF) signals are generated in the central stations, but severe constraints are thus imposed on the fiber links. One of the major problems encountered is the dispersion-induced RF power fading, which is also known as the carrier-suppression effect [4]. When using conventional intensity modulation of an optical source (Figure 1), the resulting signal consists of an optical carrier and two sidebands. The three spectral components of such an optical double-sideband (ODSB) signal experience different propagation speeds in the fiber. As the photo-detected RF signal results from the combination of the beating of each sideband with the optical carrier, destructive interference may cause cancellation of the power, P_{RF} :

$$P_{RF} \propto \cos^2\left(\frac{\pi L D \lambda^2 f_m^2}{c}\right), \qquad (1)$$

where D (ps/(nm km)) is the dispersion parameter, L is the fiber length, f_m is the RF carrier frequency, λ is the optical carrier wavelength, and c is the speed of light in a vacuum.

From the mid-1990s, various techniques – such as the use of chirped fiber-Bragg gratings (FBG) [5, 6] – have been proposed in order to compensate for, or to mitigate, this transmission penalty. It is also possible to take advantage of the optical single-sideband (OSSB) format, the chirp effect in optical modulators, or optical phase conjugation (OPC). This paper reviews most of these techniques involving schemes based on external optical modulators, optical filtering, and nonlinear effects.

2. Single-Sideband Transmission Schemes

The generation of an optical single-sideband signal with carrier (OSSB+C) – instead of the conventional optical double-sideband signal – eliminates the power-fading phenomenon, since the detected RF power results from only one beat signal. Eliminating one of the two sidebands

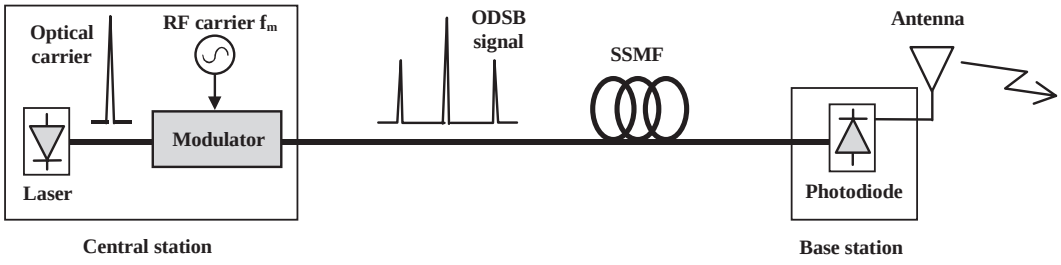

Figure 1. A fiber-radio link implementing conventional intensity-modulation and direct photo detection. Such a transmission scheme may be confronted with severe penalties due to the chromatic-dispersion effect undergone by the optical double-sideband (ODSB) signal in the standard single-mode fiber.

D. Hervé and E. Vourc'h are with the Laboratoire d'Electronique et des Systèmes de Télécommunications, UMR CNRS 6165, GET / ENST Bretagne, Technopôle Brest-Iroise, CS83818, 29238 BREST Cedex 3, France; E-mail: didier.herve@enst-bretagne.fr.
J. L. Corral, J. M. Fuster, J. Herrera, A. Martínez, V. Polo, F. Ramos, and J. Martí are with the Fibre-Radio Group, Nanophotonics Technology Centre, Universidad Politécnica de Valencia, Campus del Camino de Vera, s/n 46022 Valencia, Spain; E-mail: vpolor@upvnet.upv.es.

Editors Note: This is one of the invited *Reviews of Radio Science*, from Commission D.

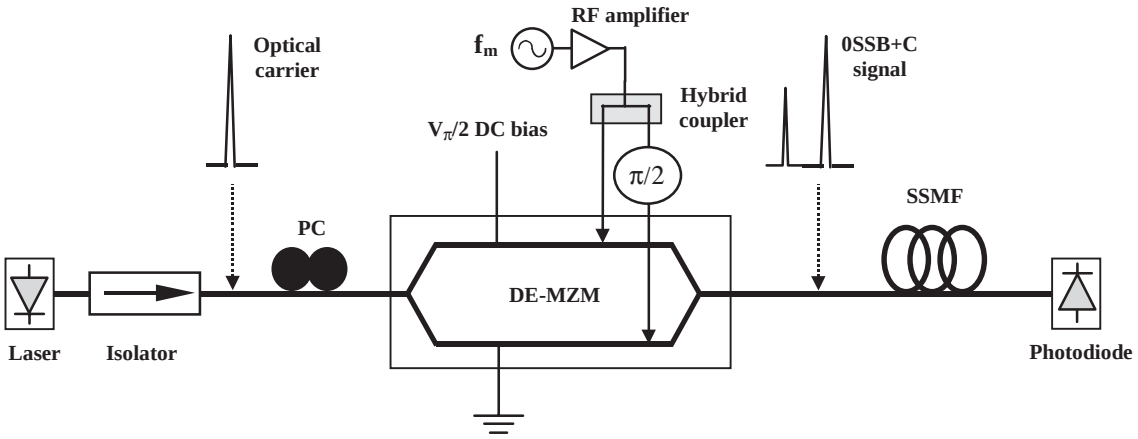

Figure 2. The experimental setup of the optical single-sideband-with-carrier (OSSB+C) source, based on a dual-electrode Mach-Zehnder modulator (DE-MZM).

of the optical spectrum can be obtained by optical filtering [7-10], or by implementing the Hilbert transform in the optical domain. Several schemes involve a dual-electrode Mach-Zehnder modulator (DE-MZM) [11], two electro-absorption modulators (EAM) in tandem configurations [12], or two cascaded phase modulators and intensity modulators [13]. Other proposed arrangements consist in incorporating a dual-electrode Mach-Zehnder modulator within a Sagnac interferometer [14, 15], implementing optical SSB modulation with suppressed carrier (OSSB+SC). Unlike other dispersion-compensation principles, the optical single-sideband signal with carrier format is independent of the fiber length and of its dispersion parameter.

In this section, four types of optical single-sideband techniques are described, showing the experimental setups that include either special external modulation arrangements or optical filtering.

2.1 OSSB+C Source Based on a Dual-Electrode Mach-Zehnder Modulator

In the source proposed by Smith et al. [11], a distributed-feedback (DFB) laser feeds a dual-electrode Mach-Zehnder modulator, biased at half its V_π switching voltage, which is also known as the quadrature-bias (QB) point. The RF signal is first divided into two parts, one of which is phase shifted by 90°, and applied to the electrodes (Figure 2). This work has shown a 1.5 dB maximum RF power degradation as a function of the applied RF signal in the 0-20 GHz range after optical single-sideband signal with carrier transmission through 79.6 km of standard single-mode fiber (SSMF). In addition, Smith et al. validated their technique by a dispersion-compensated broadband millimeter-wave (38 GHz) fiber-wireless transmission system [16]. Using this technique, the carrier suppression effect is completely overcome, but non-linear effects must be carefully considered [17].

A modification of the arrangement shown in Figure 2 has been recently proposed [18] that makes it possible to transmit the same information simultaneously at baseband or intermediate frequency (IF) and modulated onto an RF carrier, for instance at 40 GHz [19]. This scheme is dispersion tolerant and it has a remote local oscillator (LO) signal, thus alleviating the hardware requirements at the base station [22].

2.2 Integrated Lightwave Millimetric OSSB+C Source

Vergnol et al. proposed an indium phosphide (InP) integrated alternative [12] to the previous hybrid optical single-sideband signal with carrier source using a dual-electrode Mach-Zehnder modulator. It is to be noted that the integrated configuration is different from the hybrid configuration, since it comprises a distributed-feedback laser, two 40 GHz bandwidth electro-absorption modulators, a semiconductor optical amplifier (SOA), and two multimode interferometer (MMI) couplers (Figure 3). The laser provides an optical carrier that is divided into two signals of equal amplitudes, but optically phase shifted $\pi/2$ by means of a two-by-two multimode-interferometer coupler. Each output arm of the coupler feeds a high-speed electro-absorption modulator (EAM). These modulators are driven by electrical signals that originate from the same RF source, but are phase shifted by $\pi/2$. Finally, a two-by-one multimode-interferometer coupler combines the two modulated optical signals, giving an optical single sideband with carrier signal. Experimental validation of this device has shown fading-free transmission of a 38 GHz RF signal through a 50 km standard single-mode fiber link. The ripple of the photo-detected power level along the fiber proved to be as low as 2 dB. Compared with a hybrid source, the main advantage of the InP integrated device is its compactness.

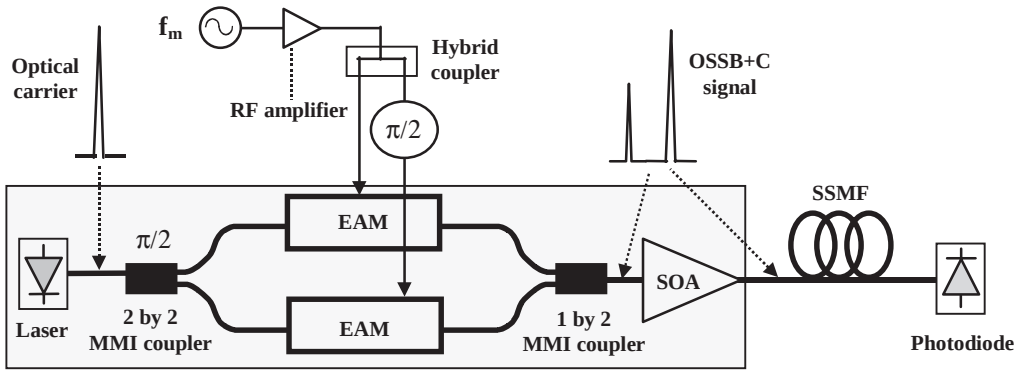

Figure 3. The experimental setup of the integrated optical single-sideband-with-carrier (OSSB+C) source

2.3 OSSB Signal Generation Implementing a Bragg Grating

The simplest way to generate an optical single sideband with carrier signal relies on the suppression of one of the sidebands of an optical double sideband signal by means of an optical filter. Such filtering was first applied to baseband digital transmission with a view toward compensating for chromatic dispersion in long-distance digital transmissions [7]. Then, Park et al. extended optical single sideband filtering to fiber-radio systems, and used a fiber Bragg grating in order to filter out one sideband of an optical double-sideband signal (Figure 4) [8]. The transmission of a 25 GHz RF signal over a 51 km-long standard single-mode fiber link was carried out, leading to no fading of the photo-detected power level. Although it is very easy to implement, this filtering technique is dependant on the wavelength of the optical carrier, and it requires a narrow-bandwidth optical filter.

2.4 Wavelength-Self-Tunable Single-Sideband (WST-SSB) Filter

Iron-doped indium phosphide (InP:Fe) is primarily known as a semi-insulating substrate, but it is also a photorefractive crystal in the infrared. In such a material – which is electro-optic – an illumination can generate free carriers that diffuse and may be trapped in the forbidden band, thanks to iron centers. Thus, interference induces a periodic charge distribution by using counter-propagating illumination in such a crystal. The periodic space-charge field thus obtained generates a periodic refractive-index variation via the electro-optic effect. Equation (2) gives the period, Λ, of such a dynamic Bragg grating. In addition, according to the Bragg diffraction condition and Snell's law, the signal wavelength, λ_s, that will be diffracted by the index grating under an angle of incidence θ satisfies Equation (3).

$$\Lambda = \frac{\lambda_p}{2n_m}, \tag{2}$$

$$\lambda_s = \lambda_p \sqrt{1-\left(\frac{\sin\theta}{n_m}\right)^2}. \tag{3}$$

In the above equations, λ_p is the wavelength of the pump beam that generates the grating, and n_m is the medium average refractive index, which equals 3.17 for InP:Fe.

In a wavelength-self-tunable single-sideband (WST-SSB) filter (Figure 5), the input optical double-sideband signal is divided into a pump beam and a signal beam by means of a 3 dB coupler. Thanks to the reflection of the pump beam off a mirror placed behind the InP:Fe crystal, interference due to each λ_i ($i = 1, 2, 3$) pump line generates a dynamic Bragg grating, G_i. In addition, suitable adjustment of θ according to Equation (3) enables λ_1 and λ_2 signal lines to be diffracted by G_1 and G_3, respectively [9]. Thus, the output signal of the device is an optical double

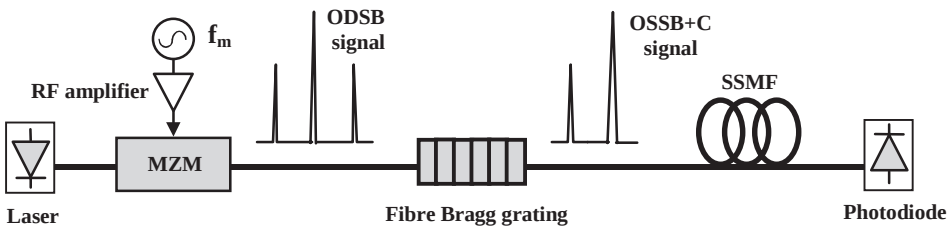

Figure 4. Optical single sideband with carrier (OSSB+C) generation implementing a fiber Bragg grating.

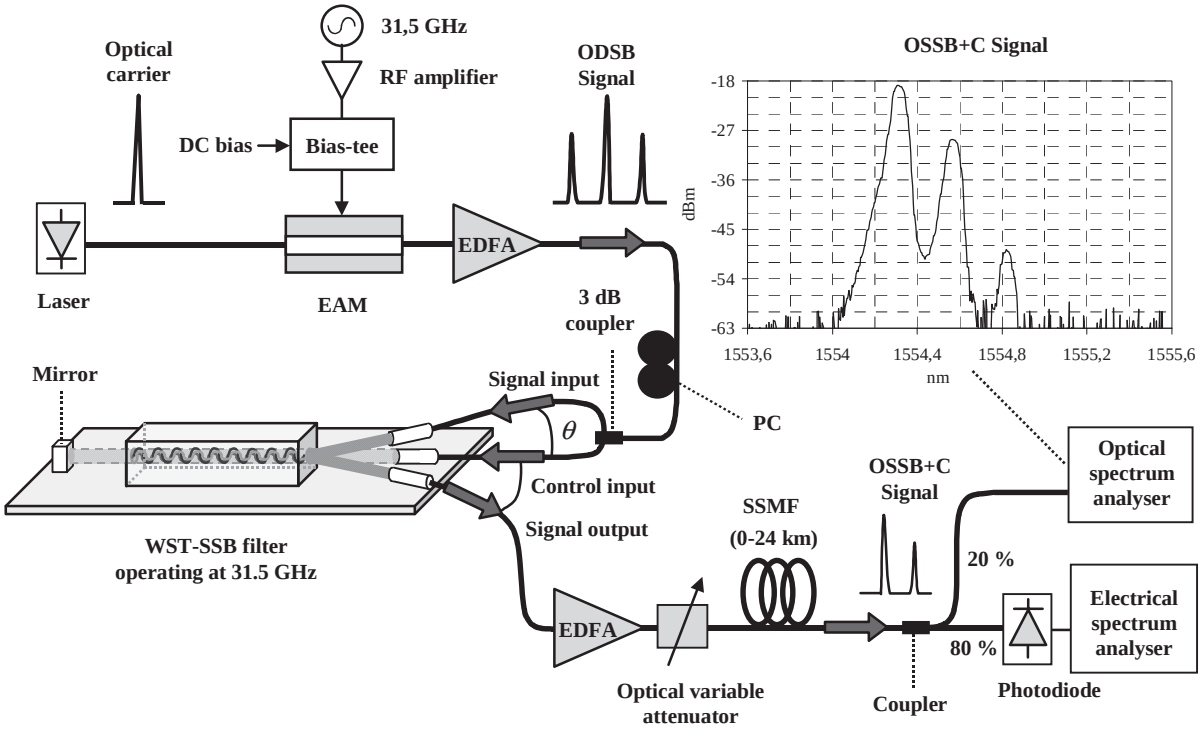

Figure 5. The experimental setup of the wavelength-self-tunable single-sideband (WST-SSB) filter and the measured output optical single sideband with carrier (OSSB+C) spectrum.

sideband with carrier (ODSB+C) signal, made up of a part of the lower sideband and carrier of the input optical double-sideband signal. Since the input signal itself generates the dynamic Bragg gratings that are responsible for its own optical single sideband with carrier diffraction, the technique has the advantage of being independent of the optical-carrier wavelength. This property makes the technique advantageous if compared to integrated optical single-sideband sources working at a given wavelength, or to optical single-sideband sources based on fixed optical filters.

Wavelength-self-tunable single-sideband filters, operating at various frequencies, were built by implementing 30 mm long photorefractive InP:Fe bulk crystals. Light was coupled into the crystal and collected at the output by means of fibered collimators. Prior to gluing all of the elements of the device onto an invar mount, micro-positioning of the collimators made it possible to adjust the θ angles so as to set the operating radio frequency of the filter.

Filters operating at 31.5 GHz RF were characterized, and the results are shown in Figure 6. In accordance with predictions, the filtered signal was actually optical single sideband with carrier. In addition, by varying the optical-carrier wavelength, the device was verified to be wavelength self-tunable. With regards to the other main characteristics of the filter, the full width at half maximum (FWHM) – which is proportional to the inverse of the grating length, L – was 1.9 GHz, the response time was of the order of a few milliseconds, and the fiber-to-fiber loss was 28 dB. The latter characteristic is imputable to the low photorefractive-effect efficiency of InP:Fe. Nevertheless, this drawback can be almost totally compensated by an erbium-doped fiber amplifier (EDFA) placed at the output of the device. Furthermore, wavelength-self-tunable single-sideband filters exhibited polarization sensitivity up to 9 dB, which is, however, not a drawback when wavelength-self-tunable single-sideband filters are transmitter devices. Finally, thanks to an extremely high upper-sideband rejection of 29 dB, the ripple of the photo-detected power level along the fiber proved to be as low as 0.8 dB.

3. Mitigation Techniques Using External Modulators

3.1 Pre-Chirping

Optical transmitters with negative chirp have been proposed to increase the frequency-length product of optical digital links, using either Mach-Zehnder electro-optical modulators (MZM) [21, 22] or electro-absorption modulators [23, 24]. In the framework of analog fiber-optic links, the interplay between the frequency chirp of the externally modulated transmitter and the fiber chromatic dispersion induces a displacement of the frequency notches of the dispersion-induced RF penalty [25] to higher frequencies, therefore increasing the −3 dB bandwidth of the link. This approach has been demonstrated employing an optical transmitter based on an electro-absorption modulator [26, 27], as shown in Figure 7. The electro-absorption modulator chirp parameter has a strong dependence on the bias voltage, and it is therefore possible

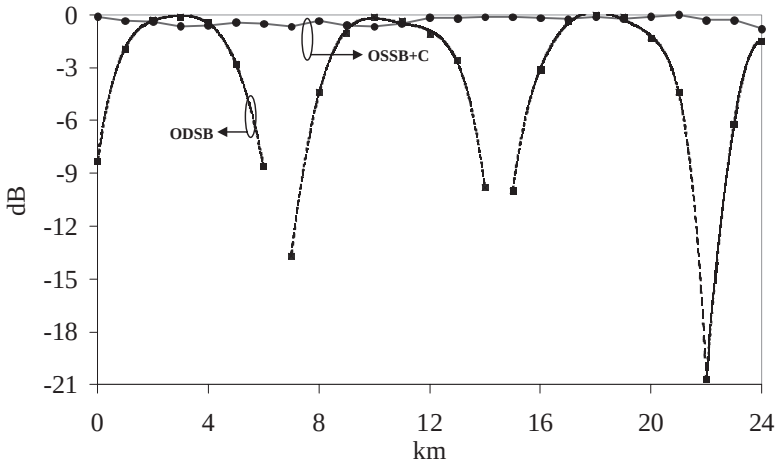

Figure 6. The relative photo-detected power level as a function of fiber length for optical double sideband (ODSB) and optical single sideband with carrier (OSSB+C) signals (modulation frequency 31.5 GHz).

to obtain negative values of this parameter for high reverse bias voltages. The photo-detected current at the output of an externally modulated analog link can be obtained as [25]

$$I_{RF} \propto \sqrt{1+\alpha^2}\cos\left[\frac{\pi LD\lambda^2}{c} f_{RF}^2 + \arctan(\alpha)\right], \quad (4)$$

where α is the chirp parameter of the transmitter, L is the link length, D is the fiber-dispersion parameter, λ is the optical wavelength, c is the speed of light in a vacuum, and f_{RF} is the frequency of the modulating signal. Figure 8 shows the experimental results obtained using the setup depicted in Figure 7, in which a continuous-wave laser was externally modulated using an electro-absorption modulator (BT Labs AT2036D2 41). The dispersion-induced RF power fading after transmission through a coil of standard single-mode fiber was measured using a light-wave component analyzer (LCA). It was demonstrated that the dispersion-induced RF power penalty frequency notches were up-shifted to higher frequencies when the electro-absorption modulator was biased at certain points of its transfer curve, resulting in negative α parameters. The theoretical results (dashed lines) agreed very well with experiments carried out for two fiber spans ($L = 25$ km and $L = 75$ km) and two electro-absorption modulator chirp parameters, $\alpha = -0.52$ and $\alpha = +1.2$, corresponding to bias points of $V_{bias} = -4$ V and $V_{bias} == 0.5$ V, respectively.

3.2 Nonlinear Optical Modulation with Suppressed Optical Carrier

The use of cascaded Mach-Zehnder modulators to implement frequency up-conversion schemes was proposed to generate and transmit millimeter-wave signals with a sharp reduction of the dispersion-induced RF power penalty [28-30]. The Mach-Zehnder modulator was biased at non-linear points of its optical transfer curve: either at the minimum-transmission bias (MITB) point or at the maximum-transmission bias (MATB) point [31, 32]. This method is limited by the high electrical power local-oscillator signal required to achieve efficient transmissions [32, 33].

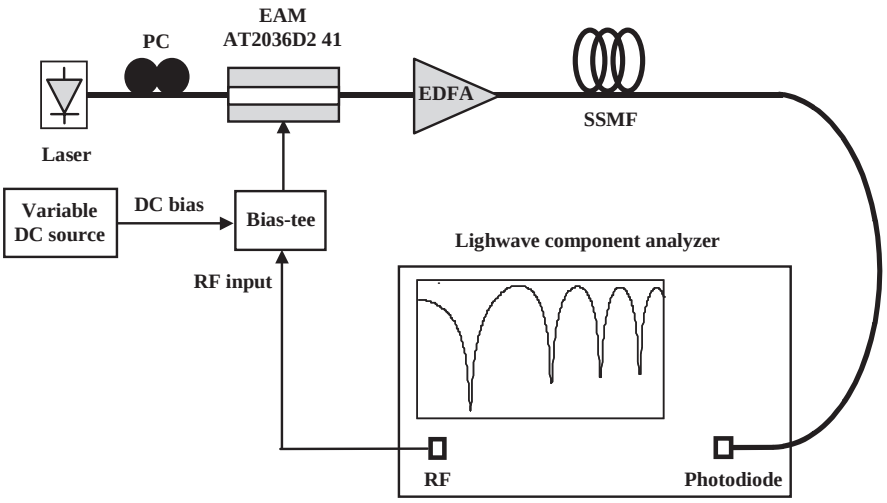

Figure 7. The experimental arrangement of an electro-absorption modulator (EAM) -based optical transmitter with adjustable chirp parameter.

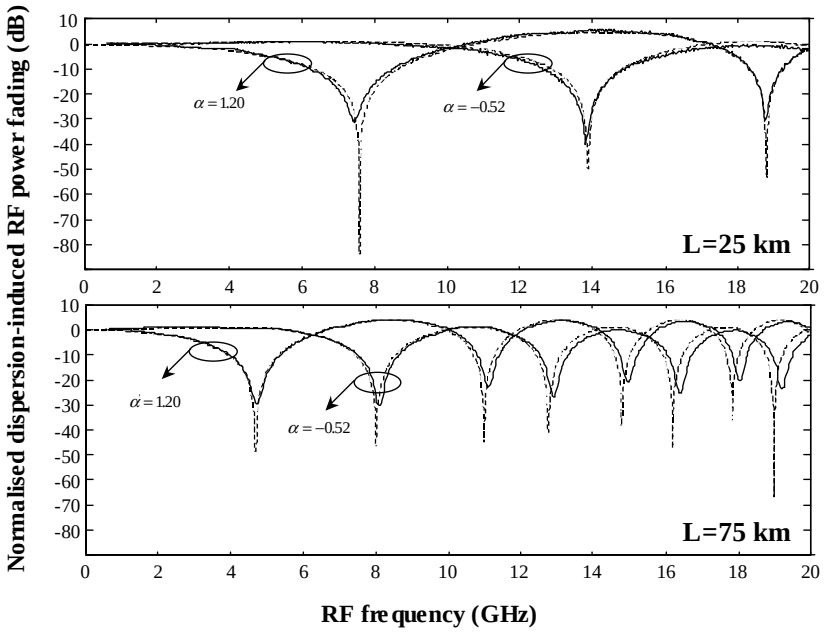

Figure 8. The theoretical (dashed) and experimental (solid) normalized dispersion-induced RF power penalty for two lengths of fiber (L = 25 km and L = 75 km) and for different chirp parameters of the electro-absorption modulator EAM (α= –0.52 and α = 1.2).

Figure 9 depicts the schematic of a photonic up-converter using two cascaded external optical modulators (EOM). The first one is used to modulate the information signal at an intermediate frequency (f_{IF}) that will be up-converted to RF using a harmonic of the local-oscillator signal. After transmission through a standard single-mode fiber, the signal at $f_{RF} = nf_{LO} + f_{IF}$ is photo detected and radiated by the base-station antenna. Depending on the chosen bias point of the local-oscillator external optical modulator, dispersion-tolerant behavior is obtained at different harmonics of the local-oscillator frequency. The right orders are $n = 2 + 4k$ for the minimum-transmission bias case, and $n = 4 + 4k$ for the maximum-transmission bias case ($k = 0,1,2,...$). Figure 10 shows the experimental verification of dispersion-tolerant transmission through a 50 km fiber-optic link of 100 MHz and 1 GHz IF tones, up-converted to frequencies of up to 12 GHz using a second harmonic of the local-oscillator signal (minimum-transmission bias case, $k = 0$). It may be observed how the carrier-suppression effect was overcome when the local-oscillator external optical modulator was biased at the minimum-transmission bias point. Similar results were obtained for the maximum-transmission bias case [31].

4. Techniques Based on Nonlinear Effects

4.1 Optical Phase Conjugation Based on Four-Wave Mixing

The feasibility of using optical phase conjugation (OPC) to compensate for the fiber-induced nonlinear distortion in cable television (CATV) networks and microwave analog systems was previously outlined in [34, 35]. Optical phase conjugation has also been demonstrated to be a powerful technique for compensating for the carrier-suppression effect that appears in optical microwave/millimeter-wave radio-over-fiber links [36-38]. The advantage of this technique with respect to others is that it also reduces the effect of fiber-induced self-phase modulation (SPM) [39], and does not impose as stringent conditions on the modulating signal as does the optical single-sideband format. The optical phase conjugation technique consists of placing an optical phase conjugator approximately at the mid-span of the optical link. Under several design constraints [39-40], the combined effects of

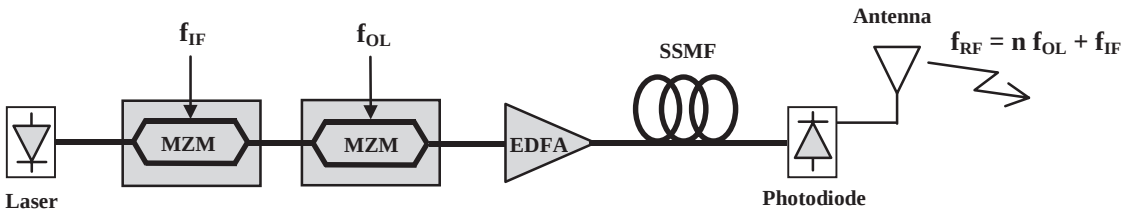

Figure 9. A schematic diagram of the photonic up-converter using two external modulators in series.

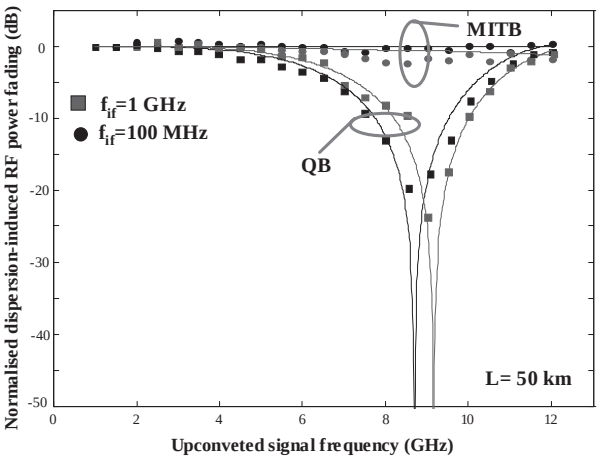

Figure 10. The dispersion-induced RF power penalty as a function of the RF frequency for the transmission of IF tones through a 50 km standard single-mode fiber fiber-optic link. The experimental results (symbols) agree very well with theory (solid lines).

chromatic dispersion and self-phase modulation, introduced by the first fiber span, may be compensated for by the following optical phase conjugation and by subsequent propagation through the second fiber span with similar characteristics.

The most common way of producing the phase-conjugated signal is by means of four-wave mixing (FWM) in a semiconductor optical amplifier (SOA) or in a dispersion-shifted fiber (DSF). Experimental results of fading-free fiber-optic transport of a millimeter-wave signal at 60 GHz, employing a semiconductor optical amplifier-based optical phase conjugation, were presented in [36]. Although the semiconductor optical amplifier-based conjugator provides a larger conversion efficiency, the dispersion-shifted-fiber based conjugator makes it possible to produce a larger input signal power without distortion, and a higher signal-to-noise ratio (SNR) may therefore be achieved [41].

The experimental arrangement used to demonstrate the compensation for the carrier-suppression effect by means of four-wave mixing in a dispersion-shifted fiber is depicted in Figure 11. A tunable laser, operating at 1551 nm, provides the optical carrier. The Mach-Zehnder modulator (MZM) output, with an optical power of 0 dBm, is launched into 25 km of standard single-mode fiber. To compensate for the chromatic dispersion effects of the first 25 km standard single-mode fiber span, a dispersion-shifted fiber-based optical phase conjugation is placed at the mid-span of the optical fiber link. The optical phase conjugation converts the input signal into a phase-conjugated replica by means of four-wave mixing through 12.7 km of dispersion-shifted fiber. The pump laser has an optical power of +3 dBm and is tuned to the zero-dispersion wavelength of the dispersion-shifted fiber (1550 nm). The pump wave and the transmitted wave are combined and amplified to induce nonlinear effects in the dispersion-shifted fiber. The same polarization state is obtained for the two waves by using a polarization controller (PC). The phase-conjugation efficiency is inversely proportional to the pump power, and is also dependent on the dispersion-shifted fiber's length, having an optimum at a fiber length of about 17.4 km [42] (slightly longer than our 12.7 km-length dispersion-shifted fiber). The conjugated signal at the output of the dispersion-shifted fiber is now filtered and amplified up to 0 dBm to be further transmitted through the second 25 km standard single-mode fiber span. The propagation through this second fiber span compensates for the chromatic dispersion

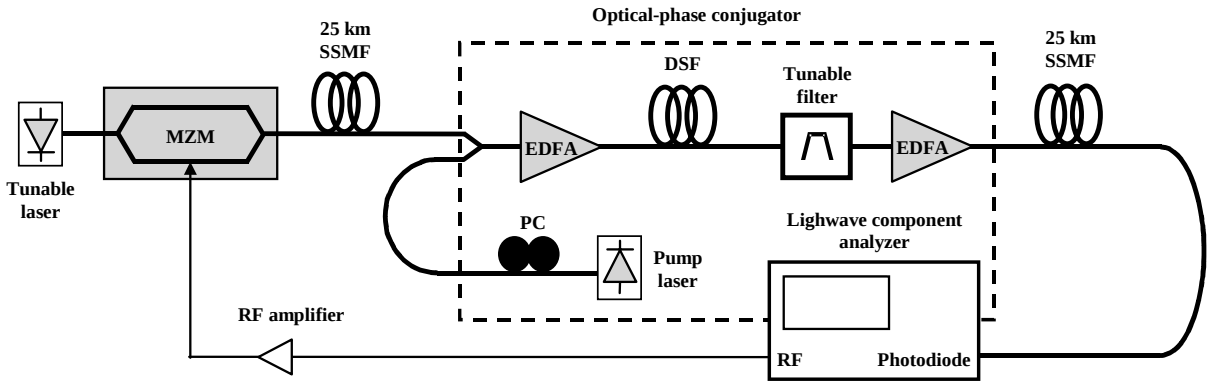

Figure 11. The experimental setup of the dispersion-shifted fiber (DSF) -based optical phase conjugation (OPC) compensation system.

accumulated at the output of the first fiber span [39]. Finally, the output of the optical fiber is photo detected, and the overall system frequency response is measured.

The simulation results of the normalized RF detected power for 50 km of standard single-mode fiber were obtained using the system model described in [35]. Figure 12 shows the cases with four-wave mixing (solid line) and without four-wave mixing (dashed line). The experimental results obtained with four-wave mixing (black circles) and without four-wave mixing (white circles) are also depicted in Figure 12, showing excellent agreement with the simulation results. The dispersion-induced power penalty was almost fully mitigated when employing dispersion-shifted-fiber-based four-wave mixing. The frequency response with four-wave mixing was nearly flat, with a variation of less than ±2 dB. This ripple was attributed to the effect of harmonics generated by the Mach-Zehnder modulator, due to the high modulation index used in the experiment (the electrical power at the RF port of the Mach-Zehnder modulator was +10 dBm). The nonlinear transfer function of the modulator and the distortion introduced by the electrical amplifier generated measured second- and third-order harmonic levels at the output of the Mach-Zehnder modulator of −30 dBc and −43 dBc, respectively, for a half-wave dc voltage of the modulator of 9 V and a modulating frequency of 2 GHz.

4.2 SOA Boosters

The use of semiconductor optical amplifiers as transmitting boosters was recently proposed to reduce the chromatic dispersion effects that occur during the fiber propagation of light in conventional microwave-optical transmissions operating near 1550 nm. It was found that the chirp introduced by the semiconductor optical amplifier under saturation conditions may be useful to mitigate the dispersion-induced effects in both digital [43] and analog [44] optical transmissions. According to a theoretical study [45], the carrier-suppression effect in conventional microwave optical links may be considerably alleviated by adjusting the semiconductor optical amplifier's input power.

The propagation of an RF externally modulated optical wave through a dispersive and nonlinear single-mode fiber in the presence of a chirp at the optical transmitter may be modeled by the frequency transfer function of a microwave optical link [46]:

$$H(z,\omega) = C_{IM-IM}(z,\omega) + \frac{1}{2} H_{PM}(\omega) C_{PM-IM}(z,\omega), \quad (5)$$

where z is the fiber distance, ω is the angular frequency, C_{IM-IM} and C_{PM-IM} are the conversion functions between intensity modulation (IM) and phase modulation (PM) in the optical fiber, and H_{PM} is the optical transmitter phase-modulation response. Furthermore, it is well known that a semiconductor optical amplifier operating under gain saturation exhibits phase modulation at its output, which may be controlled by means of the semiconductor optical amplifier's input power [43]. Therefore, it is here considered that a semiconductor optical amplifier booster be placed at the output of the optical transmitter, in order both to amplify the optical signal and to control its chirp.

In order to characterize the effect of the semiconductor optical amplifier chirp during the propagation through the single-mode fiber, the traveling-wave equations of the semiconductor optical amplifier, as given in [47], have been considered. From these equations, and assuming a small-signal approach [48], the optical-transmitter phase-modulation response may be finally expressed as [45]

$$H_{PM}(\omega) = -\alpha_N (G_0 - G)(1 + P_0/P_{sat} + j\omega\tau_c)^{-1}, \quad (6)$$

where α_N is the semiconductor optical amplifier's linewidth enhancement factor, τ_c is the carrier lifetime, P_0 is the power launched into the semiconductor optical amplifier, G stands for the saturated semiconductor optical amplifier's gain expressed in nepers, and G_0 is the unsaturated gain. The frequency transfer function of the microwave optical link may be finally obtained from Equation (5) and Equation (6).

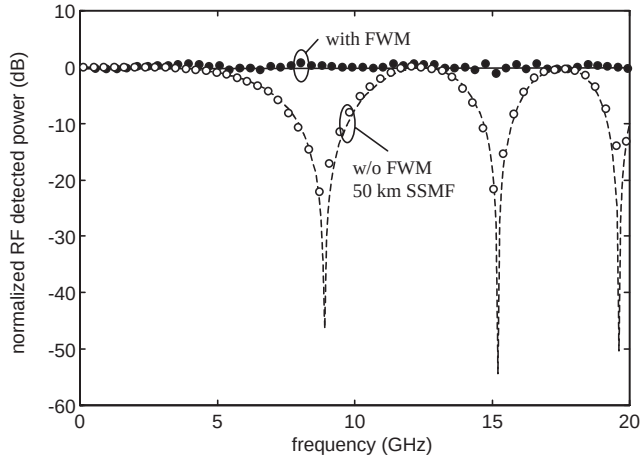

Figure 12. The simulation (lines) and experimental (symbols) results of the normalized RF detected power for a 50 km optical standard single-mode fiber (SSMF) span with four-wave mixing (FWM) (solid line and black circles) and without four-wave mixing (dashed line and white circles).

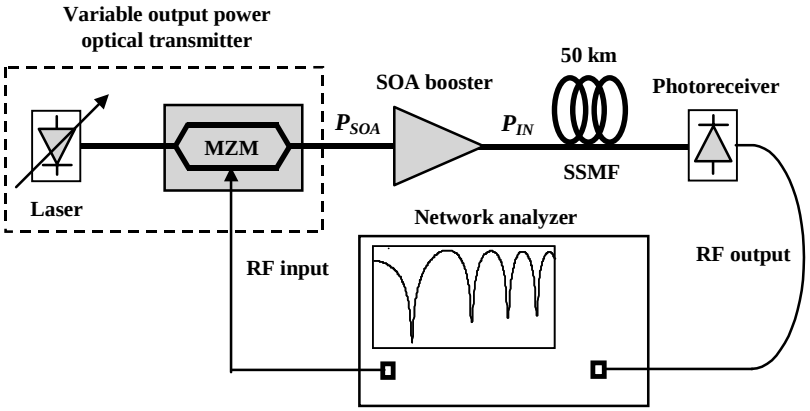

Figure 13. The experimental setup for demonstrating the reduction of chromatic dispersion effects employing a semiconductor optical amplifier (SOA) booster.

The experimental arrangement used to measure the frequency transfer function of the microwave-optical link employing a semiconductor optical amplifier booster at the optical transmitter is shown in Figure 13. An optical carrier at 1550 nm from a laser diode with variable output power was externally modulated with an RF signal, employing a chirp-free Mach-Zehnder modulator, and then amplified by the semiconductor optical amplifier booster (Philips CQF871). The variable optical power at the output of the laser, and therefore at the input of the semiconductor optical amplifier, was used to control the phase modulation and chirp at its output. The semiconductor optical amplifier output was then launched into a standard single-mode fiber of 50 km length, and finally photo detected, in order to recover the RF signal. The experimental measurements of the normalized frequency transfer function of the optical link are shown in Figure 14, up to an RF frequency of 12 GHz, under different conditions. The RF response, when no semiconductor optical amplifier was employed, exhibited deep notches. Furthermore, these notches were shifted to higher frequencies as the optical power at the standard single-mode fiber's input, P_{IN}, increased, which was due to the self-phase modulation effect [46].

On the other hand, the dispersion-induced RF carrier-suppression effect can be significantly alleviated by increasing the optical power at the semiconductor optical amplifier input, P_{SOA}, as shown in Figure 14. These RF responses were flatter for higher semiconductor optical amplifier input powers. It is to be noted that this flattening effect saturated for $P_{SOA} = +10$ dBm. The RF responses with the semiconductor optical amplifier were obtained by keeping the semiconductor optical amplifier's bias current fixed at 300 mA. As the semiconductor optical amplifier's bias current was kept constant during the measurements, the semiconductor optical amplifier experienced gain saturation when the optical power at its input was increased. The optical powers at the output of the semiconductor optical amplifier (the standard single-mode fiber input) for each measurement are also shown in Figure 14.

The measurements, which were compared with the frequency transfer function from Equation (5), are also given in Figure 14 (dashed line), and good agreement is shown. It may be may concluded that the chirp introduced by the semiconductor optical amplifier booster is useful for reducing the carrier-suppression effect and for increasing the dynamic range of analog optical links [44].

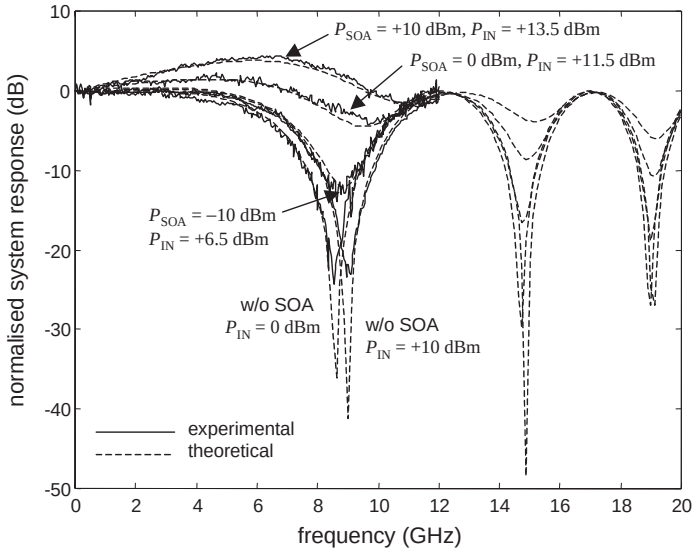

Figure 14. The normalized frequency response of the analog optical link under different conditions.

Finally, the nonlinear distortion (NLD) arising from the semiconductor-optical-amplifier-based transmitter was also measured, using both single-tone (harmonic distortion) and two-tone (third-order intermodulation distortion) driving signals at the RF port of the Mach-Zehnder modulator. For single-tone nonlinear distortion measurements, an RF tone of 6 GHz was used in the experiment. For the two-tone nonlinear distortion measurement, two RF tones of 1.9 GHz and 2.1 GHz were employed. Figure 15 shows second-order (HD2) and third-order (HD3) harmonic distortion levels as a function of the semiconductor optical amplifier's input power. The nonlinear distortion-level floor imposed by the Mach-Zehnder modulator is also depicted in Figure 15. For second-order harmonic distortion (HD2), an increase of nearly 10 dB (at +10 dBm semiconductor optical amplifier input power) was observed, owing to the semiconductor optical amplifier's nonlinear response. However, the third-order harmonic distortion (HD3) increase could be up to 15 dB, even though it was not relevant, due to the relatively high values of the second-order harmonic distortion. A third-order intermodulation distortion ($2f_2 - f_1$) level of about -52 dBc was also obtained for a semiconductor optical amplifier input power of $+10$ dBm. Therefore, the semiconductor optical amplifier's input power must be carefully controlled in order to achieve both equalization and linearity.

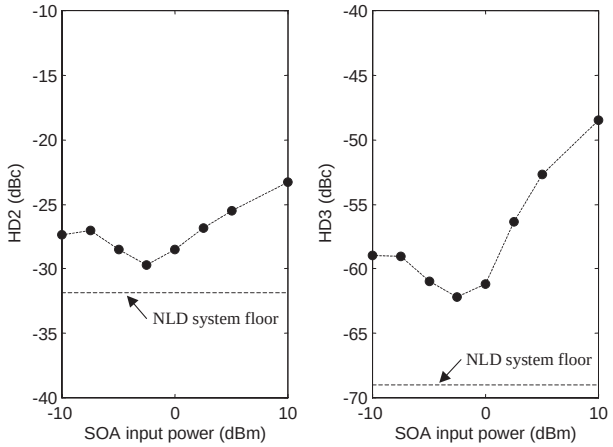

Figure 15. The harmonic distortions generated by the semiconductor optical amplifier (SOA) -based transmitter. The nonlinear distortion (NLD) system floor is shown.

5. Discussion

Several techniques to compensate for the dispersion-induced carrier-suppression effect in fiber-wireless systems have been investigated. These techniques are based on single-sideband transmission schemes, pre-chirping effects in external modulators or semiconductor optical amplifier boosters, electro-optic modulators biased at non-linear points, and optical phase conjugators. The experimental results show a good reduction – or even perfect mitigation – of the frequency notches appearing in the system's frequency response.

Numerous optical single sideband with carrier sources have been studied and reported over the past years. The technique based on a dual-electrode Mach-Zehnder modulator has the advantage of robustness and commercial availability. On the other hand, the integrated configuration is more compact, but it requires a more complex technology. Regarding the use of optical filters to remove one of the sidebands from an optical double-sideband signal, it is to be noted that such an alternative may be wavelength dependent. The impact of insertion loss and stability also has to be considered for any of the proposed configurations.

Other techniques, implementing external modulators, have been proposed. Among them, pre-chirping is a very simple approach, but the compensation is not perfect and is dependent on the link length. Chromatic dispersion effects are mitigated using the approach of nonlinear optical modulation with a suppressed carrier, enabling broad-bandwidth operation with the important advantage of harmonic generation. Nevertheless, the latter solution requires high electrical local-oscillator powers, which increase the cost and complexity of the system.

Furthermore, the use of semiconductor optical amplifier boosters significantly reduces the frequency notches (up to 20 dB), when the optical power at the semiconductor optical amplifier input is correctly adjusted to slightly saturate the semiconductor optical amplifier and control its frequency chirp. Finally, the optical phase conjugation technique makes it possible to perfectly compensate for the carrier-suppression effect, even in the presence of self-phase modulation, provided that the optical phase conjugator is correctly configured and placed at the mid-span of the fiber-optic link.

6. Conclusion

In this paper, techniques for compensating for the dispersion-induced RF power penalty that occurs in fiber-wireless transmissions have been reviewed. Many techniques have been proposed, based either on the single-sideband format, the use of external modulators, or the generation of nonlinear effects. Experimental results have demonstrated compensation for the carrier-suppression effect for frequencies well into the millimeter-wave band. This ensures the applicability of fiber-wireless techniques to next-generation broadband wireless access and transport networks.

7. List of Abbreviations

- CATV cable television
- DFB distributed feedback
- DE-MZM dual-electrode Mach-Zehnder modulator
- DSF dispersion-shifted fiber
- EAM electro-absorption modulator
- EDFA erbium-doped fiber amplifier

- EOM external optical modulator
- FWHM full width at half maximum
- FWM four-wave mixing
- HD2 2nd-order harmonic distortion
- HD3 3rd-order harmonic distortion
- IF intermediate frequency
- IM intensity modulation
- InP:Fe iron-doped indium phosphide
- LCA lightwave component analyzer
- LO local oscillator
- MZM Mach-Zehnder modulator
- MATB maximum transmission bias
- MITB minimum transmission bias
- MMI multimode interferometer
- NLD nonlinear distortion
- ODSB optical double sideband
- OPC optical phase conjugation
- OSSB optical single sideband
- OSSB+C optical single sideband with carrier
- OSSB+SC optical single sideband with suppressed carrier
- PC polarization controller
- PM phase modulation
- QB quadrature-bias
- RF radio frequency
- SNR signal-to-noise ratio
- SOA semiconductor optical amplifier
- SPM self-phase modulation
- SSMF standard single mode fiber
- WST-SSB wavelength-self-tunable single-sideband

8. References

1. D. Wake, I. C. Smith, N. G. Walker, I. D. Henning, and R. D Carver, "Video Transmission Over a 40 GHz Radio-Fibre Link," *Electronics Letters*, **28**, 21, 1992, pp. 2024-2025.

2. A. J. Seeds, "Broadband Fibre-Radio Access Networks," in *Proceedings of the International Topical Meeting on Microwave Photonics*, Princeton, USA, 1998, pp. 1-4.

3. A. Nirmalathas, C. Lim, D. Novak, and R. B. Waterhouse, "Progress in Millimetre-Wave Fiber-Radio Access Networks," *Annals of Telecommunications*, **56**, 1-2, 2001, pp. 27-38.

4. H. Schmuck, "Comparison of Optical Millimetre-Wave System Concepts with Regard to Chromatic Dispersion," *Electronics Letters*, **31**, 21, 1995, pp. 1848-1849.

5. J. Marti, J. M. Fuster, and R. I. Laming, "Experimental Reduction of Chromatic Dispersion Effects in Lightwave Microwave/Millimetre-Wave Transmissions Using Tapered Linearly Chirped Fibre Gratings," *Electronics Letters*, **33**, 13, 1997, pp. 1170-1171.

6. S. A. Havstad, A. B. Sahin, O. H. Adamczyk, Y. Xie and A. E. Willner, "Distance-Independent Microwave and Millimeter-Wave Power Fading Compensation Using a Phase Diversity configuration," *IEEE Photonics Technology Letters*, **12**, 8, 2000, pp. 1052-1054.

7. K. Yonenaga and N. Takachio, "A Fiber Chromatic Dispersion Compensation Technique with an Optical SSB Transmission in Optical Homodyne Detection Systems," *IEEE Photonics Technology Letters*, **5**, 8, 1993, pp. 949-951.

8. J. Park, W. V. Sorin, and K. Y. Lau, "Elimination of the Fibre-Chromatic Dispersion Penalty on 1550 nm Millimetre-Wave Optical Transmission," *Electronics Letters*, **33**, 6, 1997, pp. 512-513.

9. E. Vourc'h, D. Le Berre, and D. Hervé, "Lightwave Single Side-Band Wavelength Self-Tunable Filter Using an InP:Fe Crystal for Fiber-Wireless Systems," *IEEE Photonics Technology Letters*, **14**, 2, 2002, pp. 194-196.

10. J. Capmany, D. Pastor, P. Munoz, B. Ortega, S. Sales, and A Martinez, "**Multiwavelength Optical SSB Generation for Dispersion Mitigation in WDM Fibre Radio Systems Using AWG Multiplexer,"** *Electronics Letters*, **38**, 20, 2002, pp. 1194-1196.

11. G. H. Smith, D. Novak, and Z. Ahmed, "Overcoming Chromatic-Dispersion Effects in Fiber-Wireless Systems Incorporating External Modulators," *IEEE Transactions on Microwave Theory and Techniques*, **MTT-45**, 8, 1997, pp. 1410-1415.

12. E. Vergnol, F. Devaud, D. Tanguy, and E. Pénard, "Integrated Lightwave Millimetric Single Sideband Source: Design and Issues," *IEEE Journal of Lightwave Technology*, **16**, 7, 1998, pp. 1276-1284.

13. B. Davies and J. Conradi, "Hybrid Modulator Structures for Subcarrier Optical Single Sideband," *IEEE Photonics Technology Letters*, **10**, 4, 1998, pp. 600-602.

14. M. Y. Frankel and R. D. Esman, "Optical Single-Sideband Suppressed-Carrier Modulator for Wide-Band Signal Processing," *IEEE Journal of Lightwave Technology*, **16**, 5, 1998, pp. 859-863.

15. A. Loayssa, D. Benito, and M. J. Garde, "Single-Sideband Suppressed-Carrier Modulation Using a Single-Electrode Electrooptic Modulator," *IEEE Photonics Technology Letters*, **13**, 8, 2001, pp. 869-871.

16. G. H. Smith and D. Novak, "Broadband Millimeter-Wave (38 GHz) Fibre-Radio System Using Electrical and Optical SSB Modulation to Overcome Dispersion Effects," *IEEE Photonics Technology Letters*, **10**, 1, 1998, pp. 141-143.

17. F. Ramos and J. Marti, "Comparison of Optical Single-Sideband Modulation and Chirped Fiber Gratings as Dispersion Mitigating Techniques in Optical Millimeter-Wave Multichannel Systems," *IEEE Photonics Technology Letters*, **11**, 11, 1999, pp. 1479-1481.

18. V. Polo, A. Martinez, J. Marti, F. Ramos, A. Griol, and R. Llorente, "Simultaneous Baseband and RF Modulation Scheme in GBit/s Millimetre-Wave Wireless Fibre Networks," *Proceedings of the International Topical Meeting on Microwave Photonics*, Oxford, UK, 2000, pp. 168-171.

19. A. Martinez, V. Polo, J. L. Corral, and J. Marti, "**Experimental Demonstration of Dispersion-Tolerant 155-Mb/s BPSK Data Transmission at 40 GHz using an Optical Coherent Harmonic Generation Technique**," *IEEE Photonics Technology Letters*, **15**, 5, 2003, pp. 772-774.

20. A. Martinez, V. Polo, and J. Marti, "Simultaneous Baseband and RF Optical Modulation Scheme for Feeding Wireless and Wireline Access Networks*," IEEE Transactions on Microwave Theory and Techniques*, **MTT-49**, 10, 2001, pp. 2018-2024.

21. A. H. Gnauck, S. K. Korotky, J. J. Veselka, J. Nagel, C. T. Kemmerer, W. J. Minford, and D. T. Moser, "Dispersion Penalty Reduction Using an Optical Modulator with Adjust-

able Chirp," *IEEE Photonics Technology Letters*, **3**, 10, 1991, pp. 916-918.

22. J. C. Cartledge and R. G. McKay, "Performance of 10 Gb/s Lightwave Systems Using an Adjustable Chirp Optical Modulator and Linear Equalization," *IEEE Photonics Technology Letters*, **4**, 12, 1992, pp. 1394-1396.

23. J. A. J. Fells, M. A. Gibbon, I. H. White, G. H. B. Thompson, R. V. Penty, C. J. Armistead, E. M. Kimber, D. J. Moule, and E. J. Thrush, "Transmission Beyond the Dispersion Limit Using a Negative Chirp Electroabsorption Modulator," *Electronics Letters*, **30**, 14, 1994, pp. 1168-1169.

24. J. C. Cartledge and B. Christensen, "**Optimum Operating Points for Electroabsorption Modulators in 10 Gb/s Transmission Systems Using Nondispersion Shifted Fiber,"** *IEEE Journal of Lightwave Technology*, **16**, 3, 1998, pp. 349-357.

25. F. Devaux, "Optimum Prechirping Conditions of Externally Modulated Lasers for Transmission on Standard Fibre," *IEE Proceedings-Optoelectronics*, **141**, 6, 1994, pp. 363-366.

26. V. Polo, J. Marti, F. Ramos, and D. Moodie, "Mitigation of Chromatic Dispersion Effects Employing Electroabsorption Modulator-Based Transmitters," *IEEE Photonics Technology Letters*, **11**, 7, 1999, pp. 883-885.

27. A. Stöhr, K. Kitayama, and T. Kuri, "Fiber-Length Extension in an Optical 60-GHz Transmission System Using an EA-Modulator with Negative Chirp," *IEEE Photonics Technology Letters*, **11**, 6, 1999, pp. 739-741.

28. J. O'Reilly and P. M. Lane, "Remote Delivery of Video Services Using mm-Waves and Optics," *IEEE Journal of Lightwave Technology*, **12**, 2, 1994, pp. 369-375.

29. R. Hofstetter, H. Schmuck, and R. Heidemann, "Dispersion Effects in Optical Millimeter-Wave Systems Using Self-Heterodyne Method for Transport and Generation," *IEEE Transactions on Microwave Theory and Techniques*, **MTT-43**, 9, 1995, pp. 2262-2269.

30. J. M. Fuster, J. Marti, J. L. Corral, V. Polo, and F. Ramos, "Chromatic Dispersion Effects in Electro-Optical Up-Converted Millimetre-Wave Fibre-Optic Links," *Electronics Letters*, **33**, 23, 1997, pp. 1969-1970.

31. J. M. Fuster, J. Marti, J. L. Corral, V. Polo, and F. Ramos, "Mitigation of Dispersion-Induced Power Penalty in Millimetre-Wave Fibre-Optic Links," *Electronics Letters*, **34**, 19, 1998, pp. 1869-1870.

32. J. M. Fuster, J. Marti, J. L. Corral, V. Polo, and F. Ramos, "Generalized Study of Dispersion-Induced Power Penalty Mitigation Techniques in Millimeter-wave Fiber-Optic Links," *IEEE Journal of Lightwave Technology*, **18**, 7, 2000, pp. 933-940.

33. J. L. Corral, J. Marti, and J. M. Fuster, "**General Expressions for IM/DD Dispersive Analog Optical Links with External Modulation or Optical Up-Conversion in a Mach-Zehnder Electrooptical Modulator,"** *IEEE Transactions on Microwave Theory and Techniques*, **MTT-49**, 10, 2001, pp. 1968-1976.

34. J. Marti and F. Ramos, "Compensation for Dispersion-Induced Nonlinear Distortion in Subcarrier Systems Using Optical-Phase Conjugation," *Electronics Letters*, **33**, 9, 1997, pp. 792-794.

35. F. Ramos and J. Marti, "Compensation for Fiber-Induced Composite Second-Order Distortion in Externally Modulated Lightwave AM-SCM Systems Using Optical-Phase Conjugation," *IEEE Journal of Lightwave Technology*, **16**, 8, 1998, pp. 1387-1392.

36. K. Kitayama and H. Sotobayashi, "Fading-Free Fiber-Optic Transport of 60 GHz-Optical DSB Signal by Using In-Line Phase Conjugator," *Proceedings of the Optical Fiber Communication Conference*, San Diego, USA, 1999, pp. 64-66.

37. F. Ramos, J. Marti, and V. Polo, "Compensation of Chromatic Dispersion Effects in Microwave/Millimeter-Wave Optical Systems Using Four-Wave Mixing Induced in Dispersion-Shifted Fibers," *IEEE Photonics Technology Letters*, **11**, 9, 1999, pp. 1171-1173.

38. H. Sotobayashi, and K. Kitayama, "Cancellation of the Signal Fading for 60 GHz Subcarrier Multiplexed Optical DSB Signal Transmission in Nondispersion Shifted Fiber Using Midway Optical Phase Conjugation," *IEEE Journal of Lightwave Technology*, **17**, 12, 1999, pp. 2488-2497.

39. S. Watanabe and M. Shirasaki, "Exact Compensation for Both Chromatic Dispersion and Kerr Effect in a Transmission Fiber Using Optical Phase Conjugation," *IEEE Journal of Lightwave Technology*, **14**, 3, 1996, pp. 243-248.

40. S. Watanabe, G. Ishikawa, T. Naito, and T. Chikama, "Generation of Optical Phase-Conjugate Waves and Compensation for Pulse Shape Distortion in a Single-Mode Fiber," *IEEE Journal of Lightwave Technology*, **12**, 12, 1994, pp. 2139-2146.

41. H. Geiger, S. Y. Set, R. I. Laming, M. J. Cole, and L. Reekie, "Comparison of DSF- and SOA-Based Phase Conjugators Employing Noise-Suppressing Fiber," *Proceedings of the Optical Fiber Communication Conference*, Dallas, USA, 1997, pp. 150-151.

42. W. Wu, P. Yeh, and S. Chi, "Phase Conjugation by Four-Wave Mixing in Single-Mode Fibers," *IEEE Photonics Technology Letters*, **6**, 12, 1994, pp. 1448-1450.

43. T. Watanabe, N. Sakaida, H. Yasaka, F. Kano, and M. Koga, "Transmission Performance of Chirp-Controlled Signal by Using Semiconductor Optical Amplifier," *IEEE Journal of Lightwave Technology*, **18**, 8, 2000, pp. 1069-1077.

44. J. Marti, F. Ramos, and J. Herrera, "Experimental Reduction of Dispersion-Induced Effects in Microwave Optical Links Employing SOA Boosters," *IEEE Photonics Technology Letters*, **13**, 9, 2001, pp. 999-1001.

45. J. Herrera, F. Ramos, and J. Marti, "Frequency Response of Analogue Optical Links Employing SOA-Boosters," *Electronics Letters*, **38**, 19, 2002, pp. 1115-1116.

46. F. Ramos and J. Marti, "Frequency Transfer Function of Dispersive and Nonlinear Single-Mode Optical Fibers in Microwave Optical Systems," *IEEE Photonics Technology Letters*, **12**, 5, 2000, pp. 549-551.

47. A. A. M. Saleh, "Nonlinear Models of Travelling-Wave Optical Amplifiers," *Electronics Letters*, **24**, 14, 1988, pp. 835-837.

48. K. Oberman, S. Kindt, D. Breuer, and K. Petermann, "Performance Analysis of Wavelength Converters Based on Cross-Gain Modulation in Semiconductor-Optical Amplifiers," *IEEE Journal of Lightwave Technology*, **16**, 1, 1998, pp. 78-85.